Check for updates

Accepted Article

Tuning Organic Electrochemical Transistor Threshold Voltage using Chemically Doped Polymer Gates

Siew Ting Melissa Tan[1]*, *Gijun Lee*[1]*, *Ilaria Denti*[1], *Garrett LeCroy*[1], *Kalee Rozylowicz*[1], *Adam Marks*[1], *Sophie Griggs*[2], *Iain McCulloch*[2], *Alexander Giovannitti*[1^], *Alberto Salleo*[1^]

*Denotes equal contribution

[1]Department of Materials Science and Engineering, Stanford University, California 94305, USA

[2]Department of Chemistry, Chemistry Research Laboratory, University of Oxford, Oxford, OX1 3TA, UK

^Corresponding authors emails: ag19@stanford.edu, asalleo@stanford.edu

Keywords: Organic electrochemical transistor, low-voltage, stability, threshold voltage, chemical doping

Abstract

Organic electrochemical transistors (OECTs) have shown promise as transducers and amplifiers of minute electronic potentials due to their large transconductances. Tuning OECT threshold voltage is important to achieve low-powered devices with amplification properties within the desired operational voltage range. However, traditional design approaches have struggled to decouple channel and materials properties from threshold voltage, thereby compromising on several other OECT performance metrics such as electrochemical stability, transconductance, and dynamic range. In this work, we utilize simple solution processing methods to chemically dope polymer gate electrodes, thereby controlling their work function, which in turn tunes the operation voltage range of OECTs without perturbing their channel properties. Chemical doping of initially air-sensitive polymer electrodes further improves their electrochemical stability in ambient conditions. Thus, we demonstrate, for the first time,

This article has been accepted for publication and undergone full peer review but has not been through the copyediting, typesetting, pagination and proofreading process, which may lead to differences between this version and the Version of Record. Please cite this article as doi: 10.1002/adma.202202359.

This article is protected by copyright. All rights reserved.

Accepted Article

OECTs which are simultaneously low-powered and electrochemically resistant to oxidative side reactions at ambient conditions. This approach shows that threshold voltage, which was once interwoven with other OECT properties, can in fact be an independent design parameter, expanding the design space of OECTs.

Introduction

Organic electrochemical transistors (OECTs)[1] have been widely investigated in bioelectronic applications due to their ability to amplify minute potentials as well as for the biocompatibility of their active materials. Hence, OECTs have been utilized as electrodes to detect weak action potentials[2] and as ionic chemical sensors.[3] Organic mixed ionic electronic conductors (OMIECs)[4] are commonly utilized as the channel material in OECTs due to their ability to conduct both ions and electrons, as well as participate in charge transfer reactions. The recent development of polar glycol side chains in OMIECs enables the intercalation of charge-compensating counterions from the operational electrolyte into the bulk of an intrinsic polymer, enabling charge density modulations throughout the bulk.[5,6] The ability to charge volumetrically allows to widely modulate the OMIEC's charge density, and hence conductivity, using low potentials on the order of several mV. Furthermore, OECTs boast large transconductances, enabling their applications as low-powered amplifiers of minute potential perturbations, useful for the transduction of bioelectronic signals[2] and electrochemical redox reactions.[7]

OECT operation in the saturation regime is commonly described by the following equation[8,9]:

$$I_D = \mu C_c^* \frac{Wd}{2L} \frac{[V_{GS}-V_T]^2}{V_T}, |V_D| > |V_G - V_T| \qquad (1)$$

Where mobility (μ) and volumetric capacitance (C_c^*) are properties intrinsic to the channel material, *W, d,* and *L* are geometric factors of the channel, V_{GS} is the gate voltage (i.e.

This article is protected by copyright. All rights reserved.

Accepted Article

potential difference applied between the gate and source electrodes), and V_T is the threshold voltage.[1] There are several application-specific figures of merit in optimizing OECT performance such as transconductance, switching speed, turn-on voltage and electrochemical stability during operation. In particular, controlling the threshold voltage of OECTs enables the design of enhancement-mode OECTs[6,10] with turn-on voltages close to 0 V, thereby minimizing power consumption in driving circuits. Alternatively, the maximum transconductance can be optimized to occur close to 0 V,[11] thereby maximizing amplification of potentials around 0 V. The OECT's operational voltage range is determined by the threshold voltage and must be a window where the semiconductor and the electrolyte are electrochemically stable in order to ensure reliable long term operation. Importantly, electrochemical stability with respect to oxygen oxidative side reactions and low gate-source voltage operation are properties that are conventionally in contrast when using conventional gate electrodes such as Ag/AgCl. Indeed, for a given gate electrode, an OMIEC channel with a deeper highest occupied molecular orbital (HOMO), which would prevent oxidation of in air,[12] will require a higher voltage to turn on compared to an air-sensitive OMIEC with a shallower HOMO.

Several approaches have been explored to control the operating voltage range of OECTs. These approaches to control V_T however also affect the channel transport properties, which is an undesirable side-effect from the design perspective. Firstly, the OMIEC channel material can be chemically designed to have low lying energetic levels of the lowest unoccupied molecular orbitals (LUMO) and/or the HOMO. For p-type hole-transporting OMIECs, the ionization potential (IP) or HOMO level, can be increased by incorporating acceptor units[12,13] on the conjugated backbone. When utilized as the OECT channel, this shifts the threshold voltage to more negative gate voltages vs. an Ag/AgCl gate electrode.[12] While this shift is convenient as it allows to fabricate enhancement mode p-type OECTs that are chemically

This article is protected by copyright. All rights reserved.

Accepted Article

stable, it also ~~unnecessarily~~ increases the voltage requirements to switch the device ON. Furthermore, a change in molecular design of the semiconductor will affect transport properties often in unexpected ways. Alternatively, the operational voltage of the OECT can be tuned by controlling the work function of the semiconductor channel using chemical dopants. This strategy was demonstrated by introducing electron-rich amines in an initially oxidized PEDOT:PSS, essentially dedoping $PEDOT^+$ to transform the depletion mode device to enhancement mode.[14] While these approaches effectively tune the threshold voltage of the OECT, modifying the channel simultaneously changes the volumetric capacitance and charge mobility of the channel, thereby affecting the OECT's transfer characteristics and transconductance.

An alternative approach to tuning the threshold voltage while avoiding affecting the already optimized transport properties of the channel is to modify the work function of the gate electrode. One such approach is to introduce redox-active molecules in the OECT electrolyte, enabling faradaic charge transfer processes at the gate to shift its potential.[15] However, the presence of redox-active species in the OECT electrolyte may result in undesirable electron transfer reactions between the electrolyte and the channel[16] and may not be possible in all experimental conditions. In another study, metal gate electrodes with different work functions were utilized to shift the threshold voltage of the OECT.[17] To avoid parasitic side reactions, these metal electrodes must be engineered to have a large surface area or must be physically large to match the channel's large capacitance, limiting device miniaturization and integration by microfabrication. Alternatively, OMIECs could be used as the gate material due to their large volumetric capacitance. However, it has been shown that employing OMIEC as gate electrodes results in drifts in gate potential and V_T, causing drain current drift over time, in particular when the OMIEC is reactive to species in the electrolyte (e.g., molecular oxygen).[16] Other approaches to shift the operation voltage range of electrochemical

This article is protected by copyright. All rights reserved.

Accepted Article

transistors include dual-liquid-gated OECTs[18,19], tuning the channel aspect ratio[11], tuning the gate electrode capacitance,[20] self-assembled monolayers on the gate electrode,[21] and employing floating gates.[22]

In this work, we present a versatile approach to tune the OECT threshold voltage by changing the work function of OMIECs used as the gate material through chemical doping. This approach shows that V_T can be controlled as an independent parameter, decoupled from the electrochemical redox reactions of the OECT channel material, and additionally lowering OECT operating voltages. Furthermore, we are able to tune the threshold voltage of an OECT without interfering with the transport properties of the channel and achieve air-stability of the gate electrode material. We show that controlling the work function of the OECT gate enables the shifting of threshold voltages by up to 400 mV, thereby reducing its susceptibility to oxidation by ambient oxygen, improving the drain current stability of OECTs operated in ambient conditions over long periods by one order of magnitude. Finally, the use of reliable polymer-based gate electrodes enables the use of cleanroom-compatible microfabrication techniques to make scalable and stable OECTs without the need for pseudo-reference electrodes,[23] which are challenging to miniaturize and integrate.

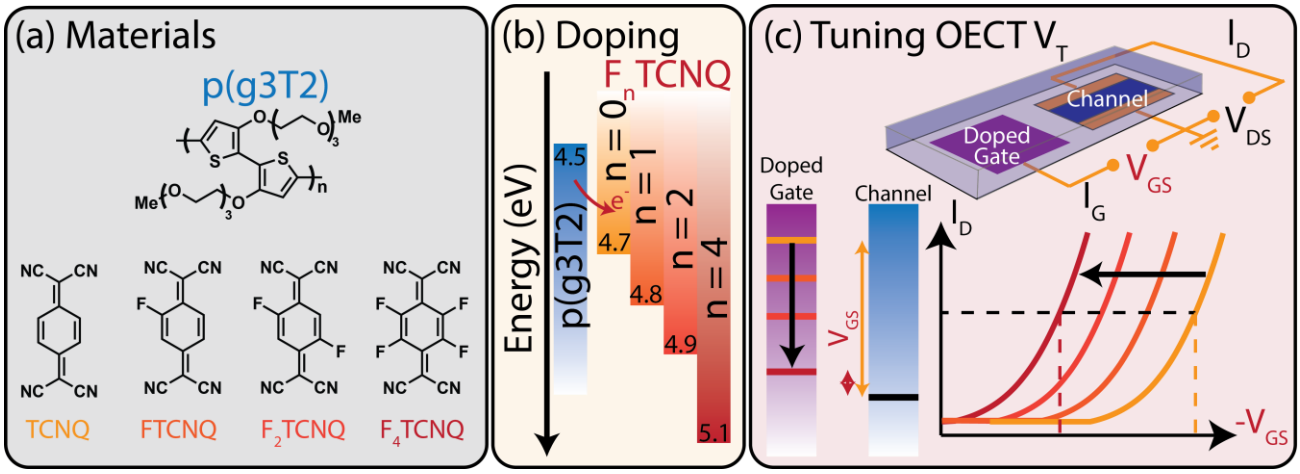

Figure 1. Concept of chemical doping of polymer gates. (a) Chemical structures of p-type polymer p(g3T2) as well as tetracyanoquinodimethane dopants with various degrees of

This article is protected by copyright. All rights reserved.

Accepted Article

fluorination (F_nTCNQ; n = 0, 1, 2, 4). **(b)** Chemical doping of p(g3T2) by dopants of various electron affinities showing electron transfer from the p(g3T2) HOMO to the LUMOs of the dopants. Energy levels of dopants vs. vacuum are estimated from cyclic voltammetry measurements (see **Fig. S1**). **(c)** Utilizing doped polymer gates of varying work functions to control the OECT threshold voltage. Top: Schematic of OECT with doped polymer gate in purple. Left: schematic of electron energy levels in gate with different dopants used and different V_{GS} required to attain the same charge state on the channel. Right: Transfer curves of OECTs with different doped gates showing the shift in threshold voltage according to the extent of doping on the gate. Note that gate voltage is shown in the negative scale to reflect the characteristics of p-type OECTs utilized in this study.

Results

To investigate the chemical tuning of gate electrodes, we studied the conjugated homopolymer with polar glycol side chains (p(g3T2))[24], which has an ionization potential (IP) of ~4.5 eV. Tetracyanoquinodimethane (TCNQ) derivatives with various extents of fluorination (F_nTCNQ; n = 0, 1, 2, 4)[25,26] were investigated as chemical dopants (**Fig. 1 (a)**). The work function of the gate electrode can be controlled by selecting the dopant of appropriate electron affinity and dopant concentration. The incorporation of fluorine atoms on TCNQ increases its electron affinity (lowering the LUMO) and hence enhances the thermodynamic driving force for extracting electrons from OMIECs with low IPs such as p(g3T2) (**Fig. 1 (b)**). The oxidation of the OMIEC gate electrode increases its work function[27] and hence shifts the OECT's threshold voltage to more positive gate voltages as depicted in **Fig. 1 (c)**.

This article is protected by copyright. All rights reserved.

Accepted Article

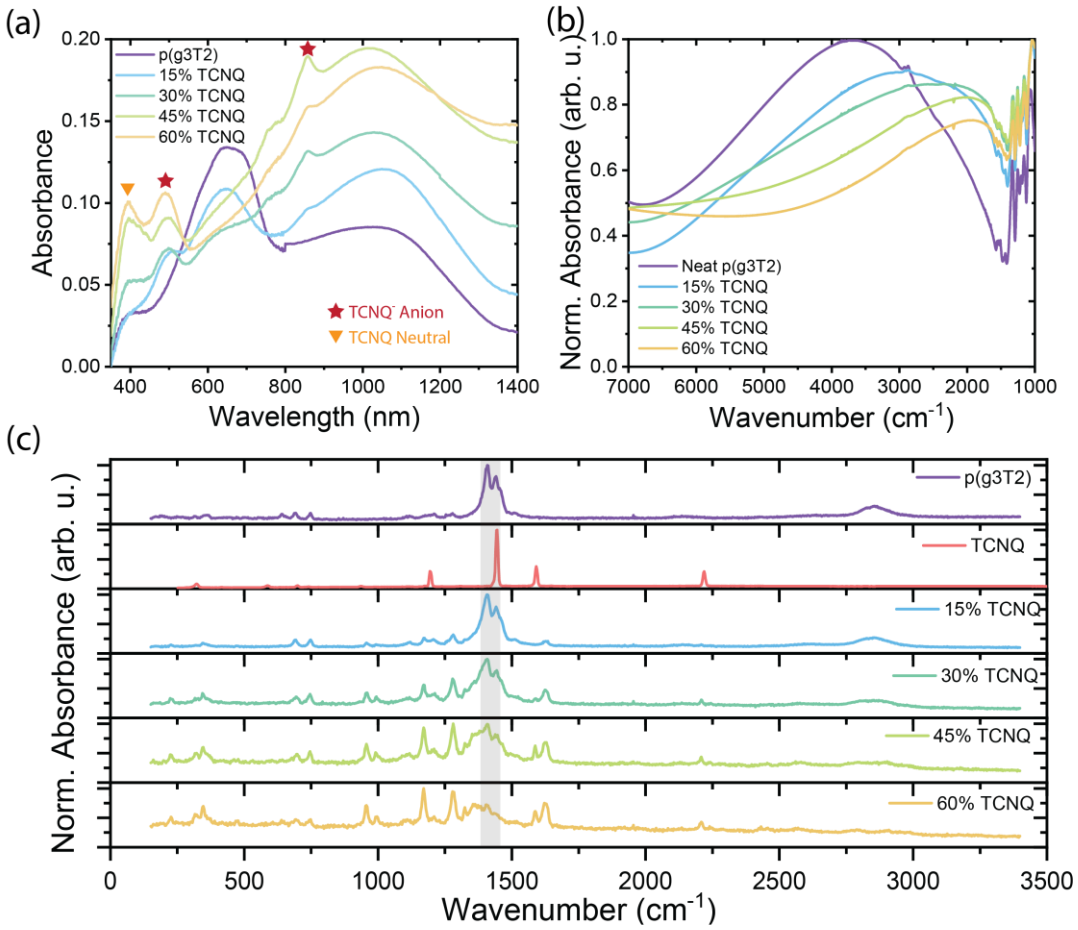

Figure 2. Characterization of neat p(g3T2) and p(g3T2) doped with 15%, 30%, 45% and 60% TCNQ prepared by solution doping. (a) UV-vis spectroscopy of p(g3T2) films on ITO/glass. Red stars and orange triangle indicate absorbance peaks of $TCNQ^-$ anion and neutral TCNQ respectively **(b)** FTIR spectroscopy of polymer films on CaF_2 substrates. **(c)** Raman spectroscopy of p(g3T2) films and neat TCNQ.

Chemically doped polymer films were prepared by mixing the polymer and the dopant in solution as described in the **Methods** section. Thin polymer films with various doping concentrations were prepared by spin coating and the extent of doping of TCNQ-doped p(g3T2) was qualitatively determined by UV-vis spectroscopy, Fourier Transform Infrared spectroscopy (FTIR), Raman spectroscopy, Photoelectron Spectroscopy in Air (PESA) as well as Grazing Incidence Wide Angle X-Ray Scattering (GIWAXS)**.** UV-vis spectroscopy of neat p(g3T2) in **Fig. 2 (a)** shows a strong absorbance around 650 nm. As the dopant concentration is increased, the intensity of the absorbance decreases due to the disappearance of neutral chains caused by the oxidation (doping) of the polymer. Simultaneously, a new

This article is protected by copyright. All rights reserved.

Accepted Article

broad absorption band appears at lower energy, evidence of hole polaron formation. This observation is corroborated by spectroelectrochemical measurements (**Fig. S2 (a)**). The absorption peaks at 500 nm and 850 nm correspond to the $TCNQ^-$ anion. These peaks gain in intensity at higher dopant concentrations, confirming electron transfer from the polymer to dopant. At higher dopant concentrations (> 45% TCNQ), an additional peak at 400 nm is observed which corresponds to unreacted neutral TCNQ. A similar observation of excess neutral dopant at high dopant concentrations was made by Kiefer et al. when doping p-type OMIECs with F_4TCNQ.[25]

FTIR spectroscopy was conducted to investigate hole polaron/bipolaron formation, which provides further evidence of oxidation of the polymer (**Fig. 2 (b)).** The broad absorbance observed in neat p(g3T2) can be attributed to polarons. As the dopant concentration is increased, this broad peak shifts to lower energy and has been previously interpreted as bipolaron formation.[28] We note that the presence of polarons in the neat polymer sample is a result of the reactivity of the polymer towards molecular oxygen when handling the polymer in ambient conditions.

Raman spectroscopy was further conducted to investigate the changes in vibrational modes of the doped polymers **Fig. 2 (c)**. The neat spectrum, which is partially oxidized at ambient conditions as explained above, is used as the reference spectrum. We assign the peaks at 1312 and 1441 cm^{-1} to the C=C antisymmetric and symmetric vibrational displacements (highlighted in grey). As the doping level increases, these peaks shift toward lower wavenumbers and lose intensity. Interestingly, the polymer sample with 15% dopant shows no sign of the neutral TCNQ molecule, indicating high conversion of the dopant to the anion. We hypothesize that the shift in the C=C vibrations for p-types could be associated with a stiffening of the backbone, as well as an increase in the planarization of the backbone.

This article is protected by copyright. All rights reserved.

Accepted Article

Morphological changes probed by GIWAXS measurements of doped p(g3T2) shown in **Fig. S3 and S4** further confirm polymer oxidation as evident from the reduction of the π-π stacking distance >45% TCNQ, in agreement with the oxidation of similar p-type bithiophene OMIECs.[25,29] At the same time, the lamellar spacing increases as dopants are likely infiltrating the side chains of the polymer. This is further supported by Raman spectroscopy where the collective vibrational displacements around the C=C peaks broaden, indicating quinoidal distortion and an increased number of configurations for the C=C vibration.

UV-vis and FTIR spectroscopy were also conducted for F_4TCNQ-doped p(g3T2) which showed greater extents of oxidation at lower dopant concentrations (**Fig. S5**), as expected due to F_4TCNQ's significantly larger electron affinity than TCNQ (**Fig. S1**). Oxidation is further confirmed by work function measurements of p(g3T2) doped with various concentrations of TCNQ and F_4TCNQ via PESA (**Fig. S6**) where p(g3T2) films doped with 60% F_4TCNQ showed up to 0.7 eV increase in work function. Due to its superior doping efficacy, F_4TCNQ doped p(g3T2) was further investigated as gate electrodes in OECT operation (**Fig. 3**).

This article is protected by copyright. All rights reserved.

Accepted Article

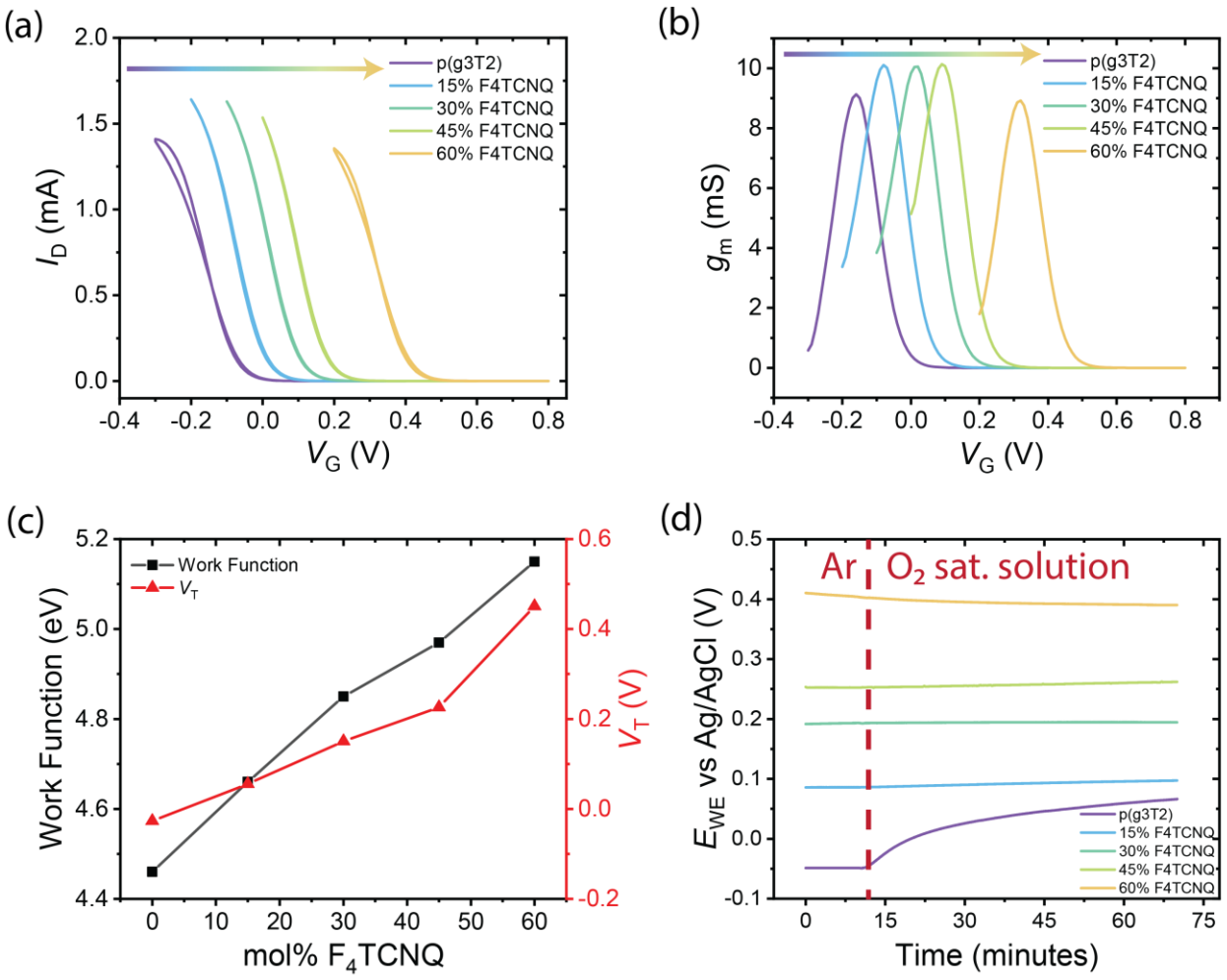

Figure 3. Controlling OECT threshold voltage by chemical doping of p(g3T2) gate electrode with F_4TCNQ (a) Transfer curves of p(g3T2) channel OECT (L=10 µm; W=2000 µm; V_D = -0.1 V, V_G scan rate of 20 mV/s) with p(g3T2) gates of various F_4TCNQ dopant concentrations **(b)** Transconductance of transfer curves shown in (a). **(c)** Plot of threshold voltage and gate work function for doped gates of different dopant concentrations. **(d)** Electrochemical stability of p(g3T2) and p(g3T2) doped with various concentrations of F_4TCNQ in Ar-saturated and O_2-saturated PBS electrolyte.

After establishing that chemical doping of p(g3T2) effectively oxidizes the polymer, we utilized these high capacitance doped polymer films as gate electrodes in OECTs (**Fig. 3 and S7-S11**). For effective comparison, identical OECT channels (materials and dimensions) were used in all measurements with different gate electrodes immersed in the electrolyte. As the p(g3T2) gate electrode becomes increasingly oxidized from increased F_4TCNQ concentration, the transfer curves shift to more positive gate voltages (**Fig. 3 (a)**). Despite the shift in transfer characteristics, the ON/OFF ratio, subthreshold swing, and maximum

This article is protected by copyright. All rights reserved.

Accepted Article

transconductance of the OECT (**Fig. 3 (a) and (b)**) remain largely unaffected by doping of the gate electrode. The correlation between the shift in gate electrode work-function, confirmed by PESA measurements (**Fig. 3 (c) and Fig. S6**) and open circuit potential vs. Ag/AgCl (**Fig. 3 (d)**), further explains the shift of the transfer curves.

The electrochemical stability of polymer gate electrodes in the presence of ambient oxygen is crucial in ensuring stable OECT operation over time.[16] To investigate this aspect, polymer electrodes with various dopant concentrations were first immersed in an Ar-saturated electrolyte followed by purging in O_2 while measuring their resting potential vs. an Ag/AgCl reference. As expected, doping p(g3T2) with F_4TCNQ significantly improves the chemical stability, limiting spontaneous oxidation reactions with molecular oxygen in ambient conditions.

(**Fig. 3 (d)**). Upon exposing neat p(g3T2) to an oxygen-saturated electrolyte, its potential increases by more than 100 mV. This observation can be explained by an electron transfer reaction from p(g3T2) to molecular oxygen, where holes are accumulated on the polymer backbone and hydrogen peroxide formation is observed as previously described for conjugated polymers with shallow IPs.[12] Chemical doping of the polymer using F_4TCNQ depletes reactive electrons from p(g3T2), making the polymer air-stable. When utilizing these air-stable chemically doped polymers as gate electrodes, an order of magnitude smaller drift of the resting potential is observed, thereby enabling steadier channel potentials and drain currents during long-term OECT operation (**Fig. S12-14**) while having negligible dissolution of dopant into the electrolyte (**Fig. S15**).

Most importantly, having a stable large work-function gate electrode provides a way to overcome the inevitable materials trade-off between channel oxidative stability (by using deep HOMO channel materials) and low gate voltage (close to 0V) operation of enhancement

This article is protected by copyright. All rights reserved.

Accepted Article

mode OECTs. Indeed, in conventional OECT design, achieving an OECT channel that is electrochemically stable in the presence of oxygen at ambient conditions (needed to achieve low OFF currents) is antithetical to low-powered devices. When operating polymers with deep HOMOs as the channel material, a large gate potential needs to be applied with respect to the commonly used gate electrode material Ag/AgCl to turn the OECT ON. Conversely, OECTs designed with $V_T \sim 0$V vs. Ag/AgCl have shallow HOMOs, such as p(g3T2), and are often susceptible to parasitic side reactions with oxygen. We demonstrate this concept by employing an air-stable polymer p(gPyDPP-MeOT2) channel (**Fig. 4 (a)**) coupled with a highly doped, air-stable gate electrode (60% F_4TCNQ-p(g3T2)). Due to its large IP of ~5.0 eV, p(gPyDPP-MeOT2) is truly an enhancement mode OECT material with low OFF currents in ambient conditions.[12] When employing a gate electrode with 60% F_4TCNQ-p(g3T2) instead of a Ag/AgCl electrode, the threshold voltage is shifted from -0.59V to -0.23V (**Fig. 4 (b) and S16**).

This article is protected by copyright. All rights reserved.

Accepted Article

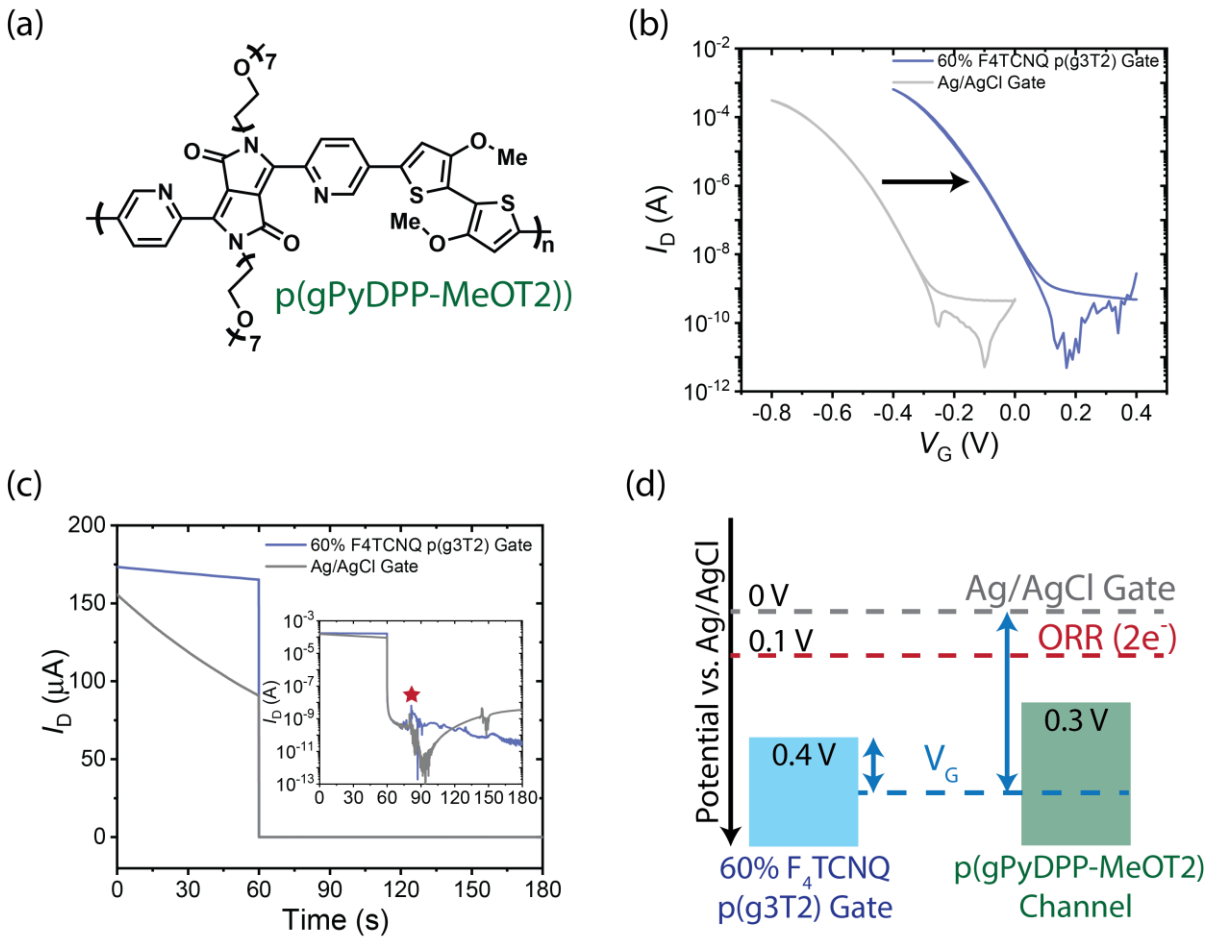

Figure 4. Low-power operation of an electrochemically stable OECT in air. (a) Structure of p(gPyDPP-MeOT2) polymer used as OECT channel **(b)** Transfer curves (L=10 μm; W=2000 μm; V_D = -0.1V with V_G scan rate of 20 mV/s) showing the shift in operational voltage of p(gPyDPP-MeOT2) channel OECT to more positive gate voltages using a doped polymer gate (60% F_4TCNQ – p(g3T2)) (shown in blue) compared to an Ag/AgCl gate electrode (shown in grey). Plot on a linear scale shown in **Fig. S16. (c)** Comparing p(gPyDPP-MeOT2) OECTs operated using different gate electrodes by measuring drain current. Blue traces: Utilizing 60% F_4TCNQ – p(g3T2) gate electrode operated from V_G = -0.4V (ON) to +0.4V (OFF). Grey traces: Utilizing Ag/AgCl gate electrode operated from V_G = -0.8V (ON) to 0V (OFF). Devices were initially ON and were turned OFF at 60s. Gate electrodes were disconnected at 80s (red star). **(d)** Energy level diagram of the HOMO of polymers, Ag/AgCl gate electrode, and oxygen reduction reaction. Blue arrows indicate the gate voltage required to charge the p(gPyDPP-MeOT2) channel.

The OECT's stability in air can be verified by measuring the drift in OFF current[12] and source potential simultaneously after disconnecting the gate electrode (**Fig. 4 (c) and Fig. S17,** see **Fig. S18** for schematic of measurement setup). We compared the stability of the OFF and ON currents of a p(gPyDPP-MeOT2) channel OECT using Ag/AgCl and 60% F_4TCNQ – p(g3T2) gate electrodes. The shift in threshold voltage from utilizing the heavily

This article is protected by copyright. All rights reserved.

Accepted Article

doped gate allows the OECT channel to be fully charged by applying V_G = -0.4V as opposed to -0.8V when utilizing an Ag/AgCl gate electrode. To verify that the channels are at similar charge states, the source potentials were measured vs. a saturated Ag/AgCl reference as shown in **Fig. S17**. After 60 seconds, both OECTs were turned OFF, resulting in source potentials between 0 to 0.05 V vs. Ag/AgCl which correspond to negligible charge states in p(gPyDPP-MeOT2) (see cyclic voltammogram in **Fig. S19 (c))**. After an additional 20 seconds, the gate electrodes were disconnected from the OECT and the channel's resting potential and drain current were monitored. While there is a small degree of potential drift on both OECT channels (**Fig. S17**), these correspond to the accumulation of minimal charge states in the polymer and therefore do not contribute to an increase in conductivity of the channel, resulting in stable OFF currents (**Fig. 4 (c)**). This shows that the electrochemical stability of an OECT channel (low OFF currents) is not affected by the choice of gate electrode. Interestingly, we also observed more stable ON currents when utilizing 60% F_4TCNQ – p(g3T2) as the gate electrode compared to Ag/AgCl. **Fig. 4 (d)** illustrates the relative energy levels of an Ag/AgCl gate electrode, oxygen reduction reaction (ORR), the oxidation onset of p(gPyDPP-MeOT2) and depleted HOMO of 60% F_4TCNQ – p(g3T2). The difference in energy levels of Ag/AgCl and 60% F_4TCNQ – p(g3T2) is approximately 0.4 V which corresponds to the difference in threshold voltage of the p(gPyDPP-MeOT2) channel OECT utilizing the two gates (-0.59V vs. -0.23V respectively). As the potentials of 60% F_4TCNQ – p(g3T2) and p(gPyDPP-MeOT2) are significantly larger than ORR, both materials are air-stable.

To illustrate the importance of selecting an air-stable channel material, we repeated the same measurements with p(g3T2) channel OECTs, which displayed significant oxidation and 10^3 increase in OFF currents upon disconnecting the gate electrode (**Fig. S17**). Hence, selecting a

This article is protected by copyright. All rights reserved.

high ionization potential channel material and using a high work function polymer gate, we can simultaneously achieve an air-stable and low-voltage OECT.

Accepted Article

This article is protected by copyright. All rights reserved.

Accepted Article

Discussion

We have shown that the chemical doping of glycolated p-type OMIEC gate electrodes with TCNQ-derivatives enables the fine tuning of the threshold voltage of OECTs by tens to hundreds of mV. This potentially enables the fine control of operational voltage range of OECTs such that it is compatible with the narrow potential ranges in bioelectronic applications. By introducing dopants to tune the energy level of OMIECs of the gate electrode, the desired gate electrode work function can be achieved. Furthermore, modifying the gate electrode effectively shifts the operation voltage range of OECTs without modifying the transport properties and electrochemical stability of state-of-the-art channel materials. As it has become common practice to utilize polymer gates for ease of processing and integration, a doped OMIEC constitutes an air-stable gate electrode that improves the operational stability of OECTs, even if the neat gate polymer was initially air-sensitive. This results stands in contrast to the frequent use of neat polymer gates which leads to current drift and operational instability. Our results show that designing OMIEC gate electrodes of large work functions improves long term operational stability in OECTs. The ability to use high work function and stable gate electrodes overcomes the previously insurmountable trade-off between channel stability in air and operation voltage in OMIECs whilst using a gate material that can be integrated in a microlithography process flow. The ability to shift V_T close to 0 V also minimizes power consumption during OECT operation. The ability to tune OECT gates using solution processing methods could open new avenues for rapid and scalable prototyping of circuits with tailored device properties via solution deposition and printing techniques. In future, this approach could also be extended to tune the operational voltage of electron-transporting OECTs to pave the way for complementary circuits where both p and n-type OECTs exhibit optimized V_T.

This article is protected by copyright. All rights reserved.

Accepted Article

Materials and Methods

p(g3T2)[24] and p(gPyDPP-MeOT2)[12] were synthesized according to literature. TCNQ and F_4TCNQ were purchased from Sigma Aldrich. FTCNQ and F2TCNQ were purchased from TCI Chemicals.

Chemical Doping

F_nTCNQ is dissolved in acetonitrile at various concentrations at 60°C for 20 minutes. 1 mg p(g3T2) is dissolved in 50 µL of chloroform at 60°C for 20 minutes. An aliquot of 150 µL F_nTCNQ solution is added to the p(g3T2) solution and stirred, followed by stirring at 60°C for 20 minutes. All procedures are done in ambient conditions. Chemical compositions of dopants are reported as mol fraction % wrt to the repeat unit of the polymer that is doped. The ease of solution processibility of both the OMIEC and dopant in miscible solvents streamlines tuning the work function of the polymer gates, enabling easier control of the doping level compared to other approaches such as vapor deposition[30,31] or solution sequential doping[30,32] of polymer electrodes.

Gate Electrode Fabrication

10 µL polymer solution was drop cast on conductive carbon paper (AvCarb P50T) and the solvent was left to evaporate at ambient conditions to form ~0.1 cm^2 electrodes. Copper tape was attached to the far end of the carbon paper electrode for electrical contact with the gate circuit.

OECT Channel Fabrication

Photolithographically patterned chips with gold contacts and patterned Parylene to expose regions for the channel were used as OECT chips[33]. p(g3T2) or p(gPyDPP-MeOT2) was dissolved in chloroform at 10 mg/mL and spin coated at 1000 rpm, annealed at 60˚C for 10

This article is protected by copyright. All rights reserved.

Accepted Article

minutes, followed by parylene lift–off to form the channel. The OECT device dimension are L = 10 μm, W = 2 mm and operated at V_D = – 0.1 V

OECT measurements

Transfer and output characteristics of the OECTs were obtained using a custom LabVIEW program with a K2612 Keithley. Gate electrodes were immersed in a PBS electrolyte.

Electrochemical Measurements

All electrochemical measurements were conducted on a Biologic SP-300 with a saturated Ag/AgCl reference electrode (BASi). Pt mesh is used as the counter electrode. Phosphate Buffered Saline aqueous solution is used as the electrolyte. Cyclic voltammetry measurements were conducted at 50 mV/s while degassing in Ar. Electrochemical Impedance Spectroscopy was conducted from 1 Hz to 100 kHz at a DC voltage set at the electrode's open circuit voltage and AC amplitude of 10 mV.

UV-vis Spectroscopy

Polymer films were spin coated on ITO/glass substrates at 1000 rpm and annealed at 60°C for 10 minutes. UV–vis spectra were taken using a Cary 6000i UV–Vis–NIR at ambient conditions.

Spectroelectrochemistry

Polymer films were spin coated on ITO/glass substrates at 1000 rpm and annealed at 60°C for 10 minutes. Wires were soldered onto ITO and insulated with epoxy and parafilm. Measurements were conducted in a quartz cuvette from Starna Cells with PBS as the electrolyte, an Ag/AgCl reference electrode and Pt mesh as the counter electrode. The electrolyte was degassed in Ar for 30 minutes prior beginning the measurements. An Ivium

This article is protected by copyright. All rights reserved.

Accepted Article

potentiostat was used to control the potential on the polymer films from -0.4V to +0.4V vs. Ag/AgCl with potential steps of 0.05V for 10 s each.[7] Spectra were acquired using QE Pro (Ocean Optics) every 1s.

Fourier-Transform Infrared (FTIR) Spectroscopy

IR absorbance spectra were collected in transmission geometry with a Thermo Scientific Nicolet iS50R FTIR, where absorbance is reported as decadic absorbance: $A = -\log_{10}(\text{Transmission})$. Spectra were collected at a spectral resolution of 0.482 cm^{-1} in the range of 700cm^{-1} to 7000cm^{-1} using a moving mirror velocity of 0.4747 cm s^{-1}. All spectra reported represent the average of 256 individual FTIR absorbance spectra. Spectra were collected with all samples in a nitrogen purged environment, and all samples were prepared by spin coating at 1000 rpm on 5 mm thick CaF_2 substrates.

Raman Spectroscopy

Polymer films were spin coated on CaF2 substrates at 1000 rpm and annealed at 60°C for 10 minutes. Raman spectra were acquired with excitation wavelength of 532nm, through the Confocal Raman microscope (XploRA, Horiba), by means of a 100x objective, in a backscattering geometry. The laser power was set at 0.13 mW to avoid sample degradation. The spectral region range was selected as 200-3400 cm^{-1}, using the 1200 gr/mm grating, in the Raman Stokes region. A silicon wafer was used for the initial calibration, through the 520.7 cm^{-1} spectral line.

Photoelectron Spectroscopy in Air

Measurements were conducted on samples spin coated on ITO/glass in a Riken AC-2 Photoelectron Spectrometer with UV illumination of 40 nW.

This article is protected by copyright. All rights reserved.

Accepted Article

Grazing Incidence Wide Angle X-Ray Scattering (GIWAXS)

Polymer films were spin coated on n++ doped Si substrates at 1000 rpm and annealed at 60°C for 10 minutes. GIWAXS measurements were conducted at 0.1° angle with 12.7 keV X-rays illuminated for 2 minutes at the 11-3 beamline at the SLAC National Accelerator Laboratory. An average of 2 images were taken per sample and data was analyzed using a combination of Nika 1D SAXS and WAXStools software packages in Igor Pro.[34,35]

This article is protected by copyright. All rights reserved.

Accepted Article

References

1. Rivnay, J. *et al.* Organic electrochemical transistors. *Nat. Rev. Mater.* **3**, (2018).

2. Khodagholy, D. *et al.* In vivo recordings of brain activity using organic transistors. *Nat. Commun.* **4**, (2013).

3. Ghittorelli, M. *et al.* High-sensitivity ion detection at low voltages with current-driven organic electrochemical transistors. *Nat. Commun.* **9**, 1–10 (2018).

4. Paulsen, B. D., Tybrandt, K., Stavrinidou, E. & Rivnay, J. Organic mixed ionic–electronic conductors. *Nat. Mater.* **19**, 13–26 (2020).

5. Moser, M. *et al.* Side Chain Redistribution as a Strategy to Boost Organic Electrochemical Transistor Performance and Stability. *Adv. Mater.* **32**, (2020).

6. Giovannitti, A. *et al.* Controlling the mode of operation of organic transistors through side-chain engineering. *Proc. Natl. Acad. Sci. U. S. A.* **113**, 12017–12022 (2016).

7. Tan, S. T. M. *et al.* High-Gain Chemically Gated Organic Electrochemical Transistor. *Adv. Funct. Mater.* **2010868**, 1–9 (2021).

8. Friedlein, J. T., McLeod, R. R. & Rivnay, J. Device physics of organic electrochemical transistors. *Org. Electron. physics, Mater. Appl.* **63**, 398–414 (2018).

9. Bernards, D. A. & Malliaras, G. G. Steady-state and transient behavior of organic electrochemical transistors. *Adv. Funct. Mater.* **17**, 3538–3544 (2007).

10. Giovannitti, A. *et al.* N-type organic electrochemical transistors with stability in water. *Nat. Commun.* **7**, 13066 (2016).

11. Rivnay, J. *et al.* Organic electrochemical transistors with maximum transconductance

This article is protected by copyright. All rights reserved.

Accepted Article

at zero gate bias. *Adv. Mater.* **25**, 7010–7014 (2013).

12. Giovannitti, A. *et al.* Energetic Control of Redox-Active Polymers toward Safe Organic Bioelectronic Materials. *Adv. Mater.* **1908047**, 1–9 (2020).

13. Krauss, G. *et al.* Polydiketopyrrolopyrroles Carrying Ethylene Glycol Substituents as Efficient Mixed Ion-Electron Conductors for Biocompatible Organic Electrochemical Transistors. *Adv. Funct. Mater.* **31**, (2021).

14. Keene, S. T. *et al.* Enhancement-Mode PEDOT:PSS Organic Electrochemical Transistors Using Molecular De-Doping. *Adv. Mater.* **32**, (2020).

15. Yu, S. & Ratcliff, E. L. Tuning Organic Electrochemical Transistor (OECT) Transconductance toward Zero Gate Voltage in the Faradaic Mode. *ACS Appl. Mater. Interfaces* **13**, 50176–50186 (2021).

16. Tan, S. T. M. *et al.* Operation mechanism of organic electrochemical transistors as redox chemical transducers. *J. Mater. Chem. C* **9**, 12148–12158 (2021).

17. Doris, S. E., Pierre, A. & Street, R. A. Dynamic and Tunable Threshold Voltage in Organic Electrochemical Transistors. *Adv. Mater.* **30**, 1–5 (2018).

18. Zhang, Y. *et al.* Liquid-Solid Dual-Gate Organic Transistors with Tunable Threshold Voltage for Cell Sensing. *ACS Appl. Mater. Interfaces* **9**, 38687–38694 (2017).

19. Ji, J. *et al.* Dual-liquid-gated electrochemical transistor and its neuromorphic behaviors. *Nano Energy* **87**, 106116 (2021).

20. Koutsouras, D. A., Torricelli, F., Gkoupidenis, P. & Blom, P. W. M. Efficient Gating of Organic Electrochemical Transistors with In-Plane Gate Electrodes. *Adv. Mater. Technol.* **6**, (2021).

This article is protected by copyright. All rights reserved.

Accepted Article

21. Sensi, M. *et al.* Modulating the Faradic Operation of All-Printed Organic Electrochemical Transistors by Facile in Situ Modification of the Gate Electrode. *ACS Omega* **4**, 5374–5381 (2019).

22. White, S. P., Dorfman, K. D. & Frisbie, C. D. Label-free DNA sensing platform with low-voltage electrolyte-gated transistors. *Anal. Chem.* **87**, 1861–1866 (2015).

23. Waleed Shinwari, M. *et al.* Microfabricated reference electrodes and their biosensing applications. *Sensors* **10**, 1679–1715 (2010).

24. Moia, D. *et al.* Design and evaluation of conjugated polymers with polar side chains as electrode materials for electrochemical energy storage in aqueous electrolytes. *Energy Environ. Sci.* 1349–1357 (2019) doi:10.1039/c8ee03518k.

25. Kiefer, D. *et al.* Double doping of conjugated polymers with monomer molecular dopants. *Nat. Mater.* **18**, 149–155 (2019).

26. Kroon, R. *et al.* Polar Side Chains Enhance Processability, Electrical Conductivity, and Thermal Stability of a Molecularly p-Doped Polythiophene. *Adv. Mater.* **29**, 35–37 (2017).

27. Jacobs, I. E. & Moulé, A. J. Controlling Molecular Doping in Organic Semiconductors. *Adv. Mater.* **29**, (2017).

28. Enengl, C. *et al.* Doping-Induced Absorption Bands in P3HT: Polarons and Bipolarons. *ChemPhysChem* **17**, 3836–3844 (2016).

29. Paulsen, B. D. *et al.* Electrochemistry of Thin Films with In Situ/Operando Grazing Incidence X-Ray Scattering: Bypassing Electrolyte Scattering for High Fidelity Time Resolved Studies. *Small* **17**, 1–7 (2021).

This article is protected by copyright. All rights reserved.

Accepted Article

30. Fontana, M. T. *et al.* Evaporation vs Solution Sequential Doping of Conjugated Polymers: F4TCNQ Doping of Micrometer-Thick P3HT Films for Thermoelectrics. *J. Phys. Chem. C* **123**, 22711–22724 (2019).

31. Patel, S. N. *et al.* Morphology controls the thermoelectric power factor of a doped semiconducting polymer. *Sci. Adv.* **3**, 1–14 (2017).

32. Scholes, D. T. *et al.* The Effects of Crystallinity on Charge Transport and the Structure of Sequentially Processed F4TCNQ-Doped Conjugated Polymer Films. *Adv. Funct. Mater.* **27**, 1–13 (2017).

33. Khodagholy, D. *et al.* High transconductance organic electrochemical transistors. *Nat. Commun.* **4**, 1–6 (2013).

34. Oosterhout, S. D. *et al.* Mixing Behavior in Small Molecule:Fullerene Organic Photovoltaics. *Chem. Mater.* **29**, 3062–3069 (2017).

35. Ilavsky, J. Nika: Software for two-dimensional data reduction. *J. Appl. Crystallogr.* **45**, 324–328 (2012).

This article is protected by copyright. All rights reserved.

Accepted Article

Table of Contents

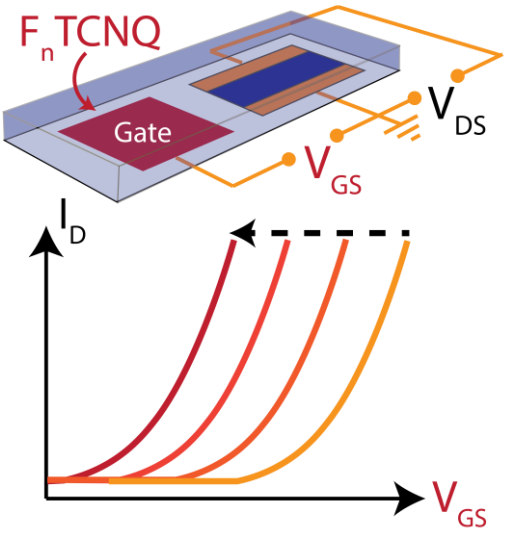

Modifying the work function of gate electrodes in organic electrochemical transistors via chemical doping makes threshold voltage an independent tunable parameter from channel properties, thereby retaining the electrochemical, transport and amplifying properties of the OECT. This enables simultaneously low-power and electrochemically stable enhancement mode OECTs.

This article is protected by copyright. All rights reserved.